(43.3 k words, 460 refs, 59 figures, 19 Tables)

Coordination-resolved electron spectroscopy of local bond relaxation and binding energy shift

Synopsis

- **Correlating STM/S, UPS, XPS, AES, APECS, and ZPS.**
- **Formulating bond relaxation and electronic binding energy associated with ill-coordinated atoms.**
- **Quantifying coordination-resolved bond length, bond energy, energy density, atomic cohesive energy, and energy levels of an isolated atom and their shifts.**
- **Clarifying physical origins and constraints in energetic spectroscopy identities as quantum entrapment and polarization.**
- **Unifying under-coordinated adatoms, defects, monolayer skins, nanocrystals, and hetero-coordinated interface and alloys.**

Complementing STM/S and U/XPS, BOLS-enabled ZPS distills atomistic, dynamic, and quantitative information of local bond relaxation and associated energetics, localization, quantum entrapment, and polarization of electrons associated with adatoms, point defects, terrace edges, monolayer skins, nanosolids, impurities, and interfaces. Derivatives resolve the performance of these ill-coordinated atoms, which dominate ubiquitously hetero-coordination Chemistry and under-coordination Physics.

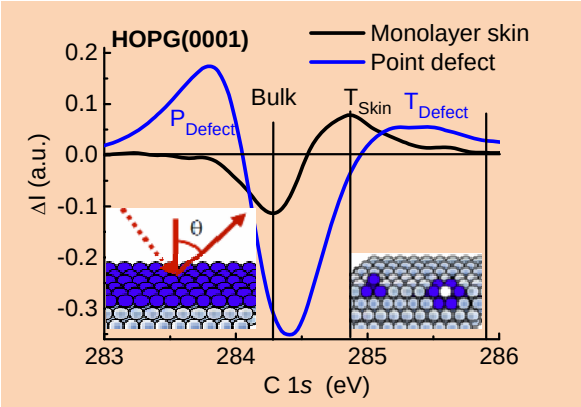

Keywords: defect, surface, impurity, interface, nanostructure, electronic structure, bond energy, STSM/S, UPS, XPS, AES, APECS, ZPS, Catalysis, entrapment, polarization

Abstract

Coordination-resolved bond relaxation in length and energy and the associated electronic dynamics pertaining to under- and hetero-coordinated atoms dictate the performance of adatoms, point defects, terrace edges, surface skins, impurities, and hetero-junction interfaces, as well as nanostructures of various shapes. However, extraction of such local and quantitative information from measurements remains a great challenge. This treatise aims to show the latest progress in this regard with focus on the advancement of the BOLS-TB (bond order-length-strength correlation and tight-binding approximation) approach and the theory-enabled zone-resolved photoelectron spectroscopy (ZPS) and their applications. The theory-enabled approach has enabled clarification, correlation, formulation, and quantification of the electronic binding energy that shifts with the coordination and chemical environment. Systematic analysis has been conducted on: i) Pt and Rh adatoms, W, Re, and Rh terrace edges, graphite monolayer skin and point defects; ii) layer and orientation resolved fcc(Pd, Rh, Pt, Ag, and Ir), bcc (W, Fe), and hcp(Be, Ru, Re) surfaces, iii) carbon allotropes and Si clusters; iii) Au, Ag, Cu, Ni, Pt, Pd and Rb nanoclusters as a function of size; and, iv) Ag/Pd, Cu/Pd, and Be/W interfaces. Exercises have led to quantitative information of the local bond length, bond energy, binding energy density, atomic cohesive energy, energy levels of an isolated atom and their bulk shifts. It is clarified that: i) perturbation to the Hamiltonian by the under-coordination-induced bond contraction, the hetero-coordination-induced bond nature alteration, and the polarization of the nonbonding electrons dictates intrinsically the binding energy shift; ii) the local densification and quantum entrapment results in the globally positive core level shift, of which the extent is proportional to the local bond energy relaxation; and iii) the polarization of the nonbonding states by the densely-entrapped bonding electrons screens and splits the crystal potential and hence shifts the binding energy negatively. Most strikingly, it has been clarified that: i) Pt adatoms and CuPd alloy serve as acceptor-type catalysts because of the dominance of entrapment while Rh adatoms and AgPd alloy as donor-type catalysts due to the dominance of polarization; ii) the graphitic Dirac-Fermi polarons result from the isolation and polarization of the dangling bond electrons by the densely-entrapped local bonding electrons surrounding the graphite surface defects and at the graphene zigzag edges. Findings not only demonstrate the power of the BOLS-TB-ZPS in complementing scanning tunneling spectroscopy and photoelectron emission spectroscopy but also the essentiality of the perspective of bond and non-bond formation, dissociation, vibration and relaxation and the associated dynamics and energetics of charge repopulation, polarization, densification and localization in engineering bonds and electrons towards devising functional materials.

Contents

Abstract 2

I Introduction 6

1.1 Scope 6

1.2 Overview 7

1.2.1 Coordination bonds, energetics, and electrons 7

1.2.2 Challenges faced by existing techniques 10

1.2.3 Beam energy and polar angle effects in PES 12

1.2.4 Effect of ill-coordination 12

1.2.5 Known mechanisms 16

1.3 Motivation and objectives 18

II Theory: BOLS-NEP-TB initiatives 19

2.1 Tight binding theory: E(k) dispersion 19

2.2 Hamiltonian perturbation by atomic ill-coordination 22

2.2.1 BOLS-NEP: Quantum entrapment and polarization 22

2.2.2 Undercoordination: Defects, surfaces, and nanostructures 22

2.2.3 Hetero-coordination: Impurity, interface, alloy, and compound 26

2.3 Formulation of ill-coordination effect 27

2.3.1 General expression 27

2.3.2 Point defects and shell resolved CLS 28

2.3.3 Sized clusters 29

2.3.4 Hetero-coordinated interfaces 30

2.4 Spectroscopy analysis: Constraints and extrinsic factors 31

2.5 Further derivatives: Atomic cohesive energy and local energy density and 33

2.6 Surface and interface energy 33

2.7 Valence band and nonbonding states 35

2.8 Summary 37

III Quantitative spectroscopies: Principles and strategies 37

3.1 Energy band structure 38

3.2 STM/S: Nonbonding and anti-bonding states 39

3.3 PES and AES: Valence-band evolution and CLS 40

3.4 APECS: Cooperative CLSs 41

3.5 ZPS: Local bond relaxation, entrapment, and polarization 45

3.6 Summary 46

IV Solid skins: Geometrical orientation and sublayer ordering 47

4.1 Fcc(100), (110), and (111) skins of Rh, Pd, Ir, and Al 47

4.2 Bcc(110), (110), and (111) skins of W 51

4.3 Hcp-structured Re, Be, and Ru 53

4.3.1 Be(0001), $(11\bar{2}0)$, and $(10\bar{1}0)$ 53

4.3.2 Re(0001) and Re$(12\bar{3}1)$ 55

4.3.3 Ru(0001) and $(10\bar{1}0)$ 55
4.4 *Local energy density and atomic cohesive energy* 57
4.5 Summary 59
V Adatoms, defects, and kink edges 60
5.1 Pt and Rh adatoms: Catalytic nature identification 60
5.2 Rh, W, and Re edges: entrapment and polarization 62
5.2.1 Atomic arrangement at edges 62
5.2.2 Rh(110) and (111) vicinal edges 63
5.2.3 W(110) vicinal edges: ZPS 64
5.2.4 W(110) vicinal edges: DFT 66
5.2.5 Re(0001) and $Re(12\bar{3}1)$ terrace edges 67
5.2.6 O-$Re(12\bar{3}1)$ kink states 69
5.3 Summary 70
VI Atomic clusters and nanocrystals 71
6.1 Gold 71
6.1.1 STM/S and DFT: ends and edge states 72
6.1.2 Size resolved energy shift of the valence and the 4f band 74
6.1.3 BOLS formulation 75
6.2 Silver 77
6.2.1 STM/S and DFT: Adatom polarization 77
6.2.2 Layer and orientation resolved CLS 78
6.2.3 APECS of Ag nanostructures 78
6.2.4 BOLS-TB formulation 79
6.3 Copper 82
6.3.1 STM/S, DFT, and PES: Atomic site and cluster size 82
6.3.2 APECS of Cu: Size, substrate, and temperature 83
6.3.3 BOLS formulation 85
6.4 Nickel 89
6.4.1 XANES and XPS: Shell resolved CLS 89
6.4.2 XPS and APECS: Crystal size 90
6.4.3 BOLS and ZPS derivatives 92
6.5 Silicon 94
6.5.1 Si(001) and (111) skins 95
6.5.2 Size-resolved 2p energy shift 96
6.5.3 Edge resolved CLS 97
6.6 Co, Fe, Pd, Pd crystals 98
6.6.1 Co nanoislands 98
6.6.2 Pd and Pt nanocrystals 99
6.6.3 Fe Nanocrystals 101
6.7 Summary 101
VII Carbon allotropes 102
7.1 GNR edges and vacancy defects 102

7.2 GNR number-of-layer dependence 104
7.3 BOLS-TB formulation 106
7.4 ZPS: Graphite monolayer skin and point defect 107
7.5 Edge-selective creation of Dirac-Fermi polarons 112
7.6 Summary 113
VIII Hetero-coordinated AgPd, CuPd, and BeW 113
8.1 Observations 113
8.2 UPS: valence band shift 115
8.3 XPS: Core band shift 116
8.4 *ZPS: Entrapment and polarization* 116
8.5 Local energy density, cohesive energy, and free energy 119
8.6 Catalytic nature and nuclear radiation protection 122
8.7 Summary 123
IX under- and hetero-coordination coupling 123
9.1 TiO_2 123
9.1.1 XPS: Ti(0001) surface: $E_{2p}(0)$ and $\Delta E_{2p}(12)$ 124
9.1.2 DFT derivatives 125
9.1.3 ZPS: Entrapment and polarization 126
9.1.4 Defect enhanced catalytic ability 128
9.2 ZnO 129
9.2.1 Transition from entrapment to polarization 129
9.2.2 Modulation of bandgap, workfunction, and magnetism 130
9.3 $SrTiO_3$ skin roughening 130
9.3 Summary 130
X Concluding remarks 131
Acknowledgements 133
References 133